Sulfur- and boron-containing porous donor-acceptor polymers for photocatalytic hydrogen evolution

Matthias G. Trunk,[a,b] Guiping Li,[a,b] Hüseyin Küçükkeçeci,[c] David Burmeister,[a,b] Martin Obermeier,[a] Boubacar Tanda Bonkano,[a,d] Arne Thomas,[c] Matthias Schwalbe,[a] Michael J. Bojdys*[a,b,e]*

a. Institut für Chemie, Humboldt-Universität zu Berlin, Brook-Taylor-Str. 2, 12489 Berlin, Germany

b. Integrative Research Institute for the Sciences Adlershof, Humboldt-Universität zu Berlin, Zum Großen Windkanal 2, 12489 Berlin, Germany

c. Institut für Chemie, Technische Universität Berlin, Hardenbergstr. 40, 10623 Berlin, Germany

d. Department of Physical Chemistry, Fritz Haber Institute of the Max Planck Society, Faradayweg 4-6, 14195 Berlin, Germany

e. Department of Chemistry, King's College London, Britannia House Guy's Campus, 7 Trinity Street, London SE1 1DB, United Kingdom

Keywords: Hydrogen evolution, water-splitting, microporous polymer network, donor-acceptor, triarylborane

ABSTRACT. Photocatalytic water-splitting provides a way to store solar energy as hydrogen gas, and hence, is an attractive alternative to energy-intensive electrolysis of water. Microporous polymer networks are an interesting class of heterogeneous photocatalysts due to the chemical modularity of their optically active backbone and their guest-accessible pore-structure. Photocatalytic action depends on efficient separation of photoexcited electron-hole pairs, and recently, it was discovered that this separation can be improved by incorporation of donor-acceptor motifs into the polymer backbones. While there are many examples of electron donors, there is little variety in electron acceptor motifs. Here, we present a series of microporous donor-acceptor networks that contain electron-deficient boron moieties (triarylborane) as the electron acceptors and sulfur moieties (thiophene) as the donors. Under sacrificial conditions, these sulfur- and boron-containing polymers (SBPs) show rates of hydrogen evolution up to 113.9 mmol h^{-1} g^{-1}. Conventionally used platinum co-catalyst does not contribute meaningfully to the photocatalytic action. Instead, palladium that is incorporated during the stage of polymer synthesis acts as the co-catalyst.

Hydrogen fuel cells compete with fossil fuel powered, internal combustion engines in vehicles, and they are excellent candidates for stationary power generation. On-site production of hydrogen gas is gaining importance as it remedies the need for transport of pressurized gas, which is extremely energy intensive and one of the main hazards associated with hydrogen technology. The only, currently available method to produce hydrogen sustainably is electrolysis using renewable energy. Solar power is the most abundant and most accessible source of energy on Earth, and the

cost efficiency of photovoltaics has risen dramatically over the last two decades. However, water electrolysis is an inefficient process and remains an industrial niche.

An alternative and more efficient way to produce hydrogen is by conversion of solar energy to hydrogen using a semiconducting photocatalyst without an applied electrical bias. To become industrially viable and truly sustainable, catalysts need to be stable against long-term irradiation and should be composed of earth abundant and environmentally benign elements. Those requirements are met by organic photocatalysts such as carbon nitrides and microporous polymer networks. Carbon nitride was first shown to catalyze the evolution of small amounts of hydrogen from water.[1] The efficiency of polymer photocatalysts was improved over time by the introduction of donor-acceptor interactions,[2–4] by increased conjugation between building blocks,[5] and by exfoliation of bulk catalysts to more accessible nanosheets with rates of hydrogen evolved exceeding 300 mmol h^{-1} g^{-1}.[6,7] Ideally, a sustainable catalyst should function without the addition of noble-metal co-catalysts, but the majority of current materials performs significantly worse without platinum additives. Previously, we have shown that organic photocatalysts retain a high hydrogen evolution activity in the absence of platinum only when strong intramolecular donor-acceptor interactions ensure an efficient separation of photoexcited electron-hole pairs.[2] In these examples, we achieved strong D-A interactions by direct coupling of thiophene-based donors and triazine-based acceptors. In addition, we found that highly conjugated, ordered polymer photocatalysts benefit less from co-added platinum than glassy, disordered polymers systems.[5]

Considering the rapid development of the field, the variety of electron-accepting building blocks commonly employed is surprisingly small. The electron-deficient triazine (C_3N_3) ring is widely used as an acceptor in organic photocatalysts, light emitters, and sensors, due to its ubiquitous derivatives that can be obtained easily *e.g.* by the acid-catalyzed trimerization of aromatic

nitriles.[2,5,8–11] Alternatively, the larger heptazine (C_6N_7) core can be integrated into nitrogen-bridged donor-acceptor systems.[12–14] To this date, however, only the triazine core has been directly cross-coupled with carbon-carbon bonds into photoactive materials.[2,15] Recently, sulfone oxides were introduced into hydrogen evolution photocatalysts. The sulfone oxides serve two functions: (i) they act as electron acceptors, and (ii) they improve the wettability of the aromatic polymer backbone.[4,16–19]

In this work, we integrate for the first time a readily available triarylborane-based electron acceptor into a donor-acceptor polymer photocatalyst. Tricoordinate boron features an intrinsic electron gap and an empty p-orbital on boron that enables charge-transfer interactions with adjacent aromatic substituents and gives rise to unique optical and electronic effects. For example, triarylboranes are used in organic light-emitting diodes[20] and as selective chemical sensors for fluoride ions.[21–25] Herein, we show that polymer networks based on sulfur-containing heterocyclic donors and triarylborane-based acceptors (SBPs) have a high efficiency as hydrogen evolution photocatalysts under visible-light and sacrificial conditions.

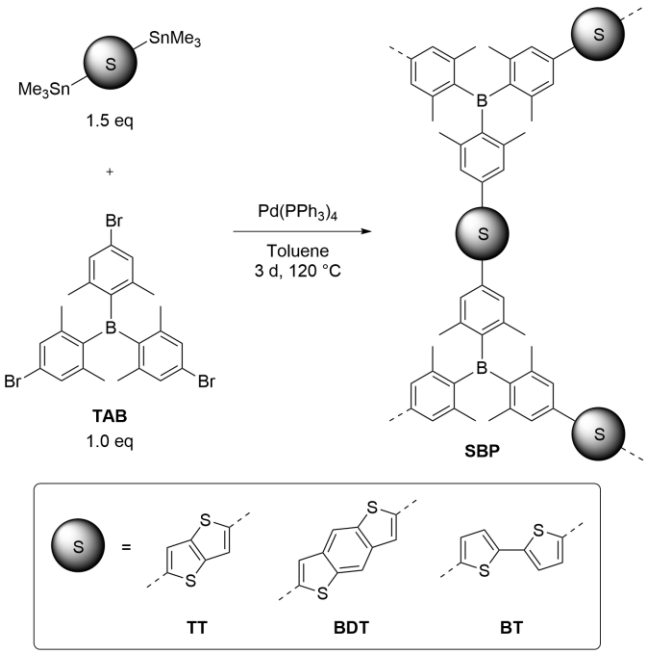

Scheme 1. Synthetic protocol to obtain sulfur- and boron-containing polymers (SBPs).

The principal borane building block used herein is accessible via commercial brominated and iodinated 1,3-dimethylbenzene. Selective lithiation of the iodide at -78 °C followed by nucleophilic attack on boron trifluoride diethyl etherate yields tris(4-bromo-2,6-dimethylphenyl)borane (TAB). The stannylated thiophene building blocks are either commercially available or synthetically accessible using a deprotonation-stannylation route. Following our reported procedure,[2] the Stille-type polymerization of C_2-symmetric donor to C_3-symmetric acceptor units in a 3:2 ratio affords powders of TT-TAB, BDT-TAB, and BT-TAB of vibrant yellow and orange colors (Scheme 1).

We performed nitrogen sorption experiments at low-temperature, and calculated the accessible surface areas according to the Brunauer-Emmett-Teller (BET) model (**Error! Reference source not found.**C and Figure S2 in the supporting information). The rigid polymer backbones of TT-TAB and BDT-TAB afford comparative large surface areas of 755 and 664 $m^2\ g^{-1}$, respectively.

BT-TAB contains bithiophene units linked by flexible, single bonds, and consequently, the material does not show significant, guest-accessible pores (BET of 66 m^2 g^{-1}).

Scanning electron microscopy (SEM) imaging reveals that all SBPs have a cauliflower-shaped morphology typically observed for materials formed via point-nucleation in irreversible coupling reactions, with particle sizes in the range of 50-100 μm (Figures S3-S5). Powder X-ray diffraction (PXRD) patterns show that these materials are completely amorphous, as expected for products of palladium-catalyzed irreversible C–C coupling reactions (Figure S8).

The chemical composition of the materials was determined by combustion elemental analysis, and the observed amounts of carbon, hydrogen and sulfur are in good agreement with the theoretical values (Table S1). The contents of boron, tin and palladium were determined via inductively coupled plasma optical emission spectroscopy (ICP-OES). The amounts of boron range between 1.50 and 1.59 wt% (inst. error ± 10%). These are slightly lower than the theoretical values (between 1.90 and 2.04 wt%) but are still commensurate considering the minuscule contribution of boron to the overall composition. Residual amounts of tin originating from unreacted end groups range between 0.01 and 0.03 wt%, corroborating the elemental analysis results and confirming a high coupling efficiency. As is common for polymer networks obtained via palladium-catalyzed cross-coupling reactions, we detected small amounts of immobilized palladium (between 1.1 and 1.5 wt%).[2,16,26] Detailed ICP-OES results can be found in the supporting information (Table S2). After thermogravimetric analysis (TGA) up to 1000 °C under oxygen atmosphere, we observe residual masses of around 6 wt% for each of the SBP samples (Figure S7). After full oxidation of carbon, sulfur and hydrogen to volatile CO_2, H_2O, and SO_3, we attribute this non-volatile residue to the expected mass of B_2O_3 including the residual mass of palladium (Table S6).

Fourier-transform infrared (FTIR) spectra show the presence of characteristic absorption peaks of the triarylborane building block in all SBP samples, and hence, they hint at successful co-polymerization (**Error! Reference source not found.**A). Additional peaks are assigned to the respective thiophene building block (Table S3-S5). ^{1}H-^{13}C solid-state cross-polarization magic angle spinning nuclear magnetic resonance (^{1}H-^{13}C CP-MAS NMR) spectra show signals between 108 and 155 ppm assigned to the arylic subunits of the triarylborane as well as thiophene-based building blocks (**Error! Reference source not found.**B). A characteristic, strong signal at 21-22 ppm originates from the methyl groups shielding the central boron atom. The ^{11}B nucleus has a half-integer spin of 3/2 and a quadrupole moment that gives rise to an unusual peak shape in solid-state NMR spectra (Figure S6). We observe this peak in the ^{11}B NMR spectra of all SBPs at around 69 ppm flanked by a number of central-transition signals that are in excellent agreement with literature.[27]

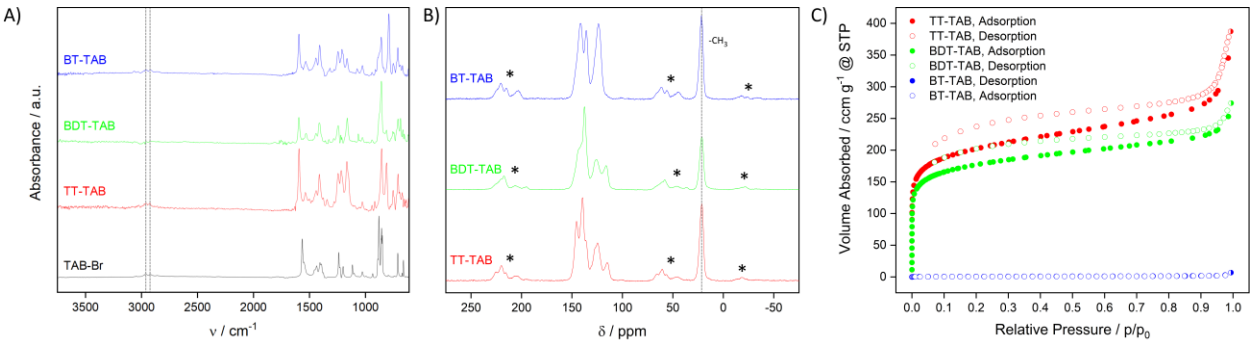

Figure 1. A) Fourier-transform infrared (FTIR) spectra for all SBPs (BT-TAB in blue, BDT-TAB in green, TT-TAB in red) as well as for their principal TAB-Br building block (in black). Dashed lines denote methyl group signals. B) ^{1}H-^{13}C cross-polarization magic-angle spinning (CP-MAS) solid-state NMR spectra for all SBPs, recorded at 8 kHz. Asterisks (*) denote spinning sidebands,

dashed lines denote methyl group signals. C) Nitrogen sorption isotherms of all SBPs, measured at 77 K.

Ultraviolet-visible (UV/Vis) reflectance spectra measured in the solid-state show that the frameworks absorb visible light up to 530 nm (**Error! Reference source not found.**A). Based on the UV/Vis spectra, the direct optical bandgaps of TT-TAB, BDT-TAB, and BT-TAB are estimated as 2.58, 2.56 and 2.49 eV, respectively (**Error! Reference source not found.**D). Therefore, all bandgaps are in the range suitable for visible-light photocatalytic proton reduction.[28]

Photocatalytic hydrogen evolution reactions were carried out using incident light above 395 nm, and the amount of evolved hydrogen was determined by injection of headspace samples into a gas chromatograph equipped with a thermal conductivity detector. To obtain sufficient dispersion of the hydrophobic SBPs in aqueous medium, the catalytic tests were performed in a solvent mixture comprising equal volumes of water and acetonitrile. To evaluate the catalytic activities, we screened different reaction parameters such as catalyst loading and type of sacrificial agents, and we found that both factors had a strong influence on the catalytic activity. The lowest tested concentration of 1 mg of catalyst per 16 mL of solvent gave the highest activity per mass of catalyst (Figure S10). Even at such low loadings, we observed vigorous formation of hydrogen bubbles (see video in the supporting information). It has been noted previously that low catalyst concentrations can result in exceptionally high catalytic activity.[29] However, despite the low catalyst loadings tested here, we observe smooth hydrogen evolution curves and good reproducibility. L-ascorbic acid, triethanolamine, and triethylamine were evaluated as sacrificial electron donors (Figure S11). Similar to other recently reported microporous polymer photocatalysts, L-ascorbic acid yielded the highest activities by far.[3,19] Using L-ascorbic acid as the sacrificial agent, TT-TAB, BDT-TAB, and BT-TAB showed hydrogen evolution rates of

113.9, 87.7, and 74.2 mmol h^{-1} g^{-1}, respectively, under addition of 3 wt% of platinum and averaged over five hours (**Error! Reference source not found.**B). No hydrogen was detected when experiments were performed without the organic catalyst, water, or sacrificial electron donor. Testing of multiple batches as well as multiple runs on the same batch confirmed the activity of the best-performing material, TT-TAB, within a 15% error margin (Figure S13).

These notable activities are corroborated by apparent quantum efficiencies (AQEs) at different wavelengths, which we determined for the most active material, TT-TAB. At wavelengths of 415, 460 and 490 nm, we obtained excellent AQEs of 4.48, 1.80, and 0.80%, respectively. These values are consistent with the acquired UV/Vis absorption spectrum of TT-TAB (Figure S15). Considering that the catalyst concentration used here is 10 to 20 times lower than in comparable systems,[2] these high efficiencies are particularly notable since AQE calculations rely on the generated amount of hydrogen molecules per incident photons without taking catalyst concentration into account.

We evaluated the photochemical stability of our best-performing SBP system, TT-TAB, in long-term hydrogen evolution experiments. Initially, TT-TAB was irradiated for four cycles each of 5 h length with hourly gas chromatography measurements. After each cycle, the initial amount of sacrificial agent was replenished by addition of solid ascorbic acid, the solvent was exchanged, and the reaction mixture was degassed thoroughly before further irradiation. Over the course of this experiment, the catalytic activity of TT-TAB remained effectively constant (**Error! Reference source not found.**F). We verified the chemical integrity of the TT-TAB polymer before and after 15 h of continuous photocatalysis using FTIR, solid-state NMR, and UV/Vis spectroscopy, and we observed no significant changes (Figure S17-S19). NOTE: without the suggested solvent exchange, we observe an accumulation of side-product from the oxidation of L-

ascorbic acid in the reaction vessel which has a detrimental effect on HER activity over time (Figure S15).

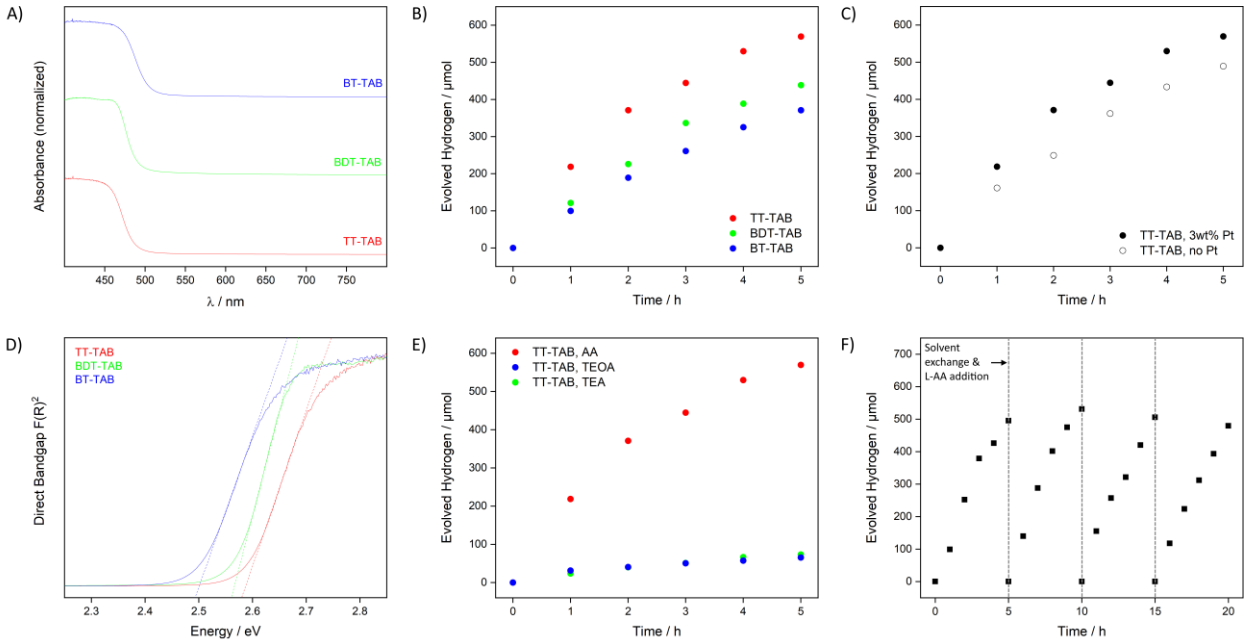

Figure 2. Optical characterization of all SBPs showing A) solid-state UV/vis spectra and D) the derived direct optical bandgaps; B) hydrogen evolution experiments comparing the activity of all SBPs with L-ascorbic acid as sacrificial agent; E) comparison of sacrificial agents using TT-TAB as catalyst; C) influence of platinum as co-catalyst; F) long-term hydrogen evolution using TT-TAB and L-ascorbic acid as sacrificial agent without added platinum. Dashed lines denote exchange of solvent and addition of fresh sacrificial agent. General conditions for HER experiments using L-ascorbic acid: 1 mg of catalyst, 8 mL acetonitrile, 8 mL L-ascorbic acid (0.1 M), platinum (3 wt%) unless marked platinum-free. Further conditions can be found in the SI.

In most polymer photocatalysts, omission of the platinum co-catalyst leads to a significant drop of the rate of hydrogen evolution (e.g., by more than 37% for similarly performant systems).[6,19]

Using TT-TAB as the photocatalyst without platinum, we observe a drop in the rate of hydrogen evolution by only 14% (from 113.9 to 97.9 mmol h^{-1} g^{-1}, **Error! Reference source not found.**C). At a rate of 74.2 mmol h^{-1} g^{-1}, the activity of BT-TAB is the lowest in our SBP series, and it remains essentially constant in the presence or absence of platinum (Figure S12).

In addition, we investigated whether the trace amounts of palladium detected by ICP-OES act as co-catalysts during photocatalysis. To that end, we treated TT-TAB with tetramethylethylenediamine (TMEDA), a potent chelating agent, to remove accessible palladium from the polymer matrix. After three days of TMEDA extraction, the palladium content in TT-TAB dropped by 28% (from 1.19 wt% to 0.86 wt% as determined by ICP-OES). Commensurately, we observed a 31% drop in the rate of hydrogen evolution using the Pd-depleted photocatalyst (Figure S16). Longer periods of TMEDA-treatment did not result in a further, significant decrease of Pd-content (up to 0.76% after six days), indicating a thermodynamic and kinetic limit to the amount of palladium which can be removed using this diffusion-controlled method. We surmise that in our SBP samples palladium assumes the role of an efficient co-catalyst, in particular, since further addition of conventionally-used platinum does not lead to significant improvement of photocatalytic action.

We propose that the comparatively high efficacy of SBPs in photocatalytic hydrogen evolution stems from their electronic make-up – in particular, from their ability to effectively separate photoexcited charge carriers. To determine the lifetime of the excited states, we performed time-correlated single-photon counting (TCSPC) experiments. The lifetimes obtained from triexponential decay fitting are similar to those of previously reported triarylborane-based donor-acceptor systems[22] and other solid donor-acceptor hydrogen evolution catalysts.[3,30] The weighted average lifetime τ_{avg} is longest for BDT-TAB (0.259 ns), followed by TT-TAB (0.180 ns) and BT-

TAB (0.104 ns). From the absolute lifetimes, we surmise that the first (τ_1) and second (τ_2) decay processes are too fast and that the excitons are too short lived to contribute significantly to the (diffusion-limited) photocatalytic process. Interestingly, however, the longest lifetime τ_3 has a similar weight in all materials (of between 4 and 7 %), and it decreases going from TT-TAB (2.960 ns) via BDT-TAB (2.000 ns) to BT-TAB (0.920 ns). This lifetime decrease follows the same trend as the observed catalytic activities (with TT-TAB as highest, and BT-TAB as lowest) (Figure S21 and Table S7).

To obtain a qualitative understanding of the donor-acceptor interactions in our polymers, we performed density functional theory (DFT) calculations of the frontier orbitals in a model system. This model comprises the triarylborane core connected to three thiophene moieties and represents a large segment of the polymeric repeats common to all three SBPs. The obtained Kohn-Sham highest occupied molecular orbital (HOMO) shows a node on the boron atom, whereas the lowest unoccupied molecular orbital (LUMO) has a large coefficient on boron, and notably smaller coefficients on the other atoms (Figure S22). From these results we conclude that, after vertical excitation, the excited electron has the highest probability density at the boron center. On the basis of these calculations, we propose the following mechanism for photoexcitation and hydrogen evolution: (i) photoexcited charges separate and form a boryl radical anion and thiophene radical cation, and (ii) the generated cation is reduced by single-electron transfer from ascorbate. (iii) A second photoexcitation event transfers another electron to the boron center and the emerging electron pair is protonated, forming a borohydride species. Finally, (iv) a second proton induces elimination of hydrogen (H_2) and the catalyst regenerates via a second, single-electron transfer from ascorbate (Figure S23). We are aware that this proposed mechanism does not account for the role of Pd co-catalyst and that further studies on the mechanism are required to make a definitive

statement. To a first approximation, Pd co-catalyst separates photoexcited electron-hole pairs spatially and for long enough to become photocatalytically active.

In summary, we have synthesized a series of highly active hydrogen evolution polymer photocatalysts that contain sulfur and boron moieties (SBPs), and in doing so, we introduced a readily available electron acceptor, triarylborane, to the library of building blocks for visible-light photocatalysts. Under optimized conditions, the thieno[3,2-*b*]thiophene-triarylborane copolymer (TT-TAB) produces 113.9 mmol of hydrogen per hour per gram of catalyst. Most importantly, even without added platinum co-catalyst, its activity is close to 100 mmol h^{-1} g^{-1}, a benchmark value. These findings emphasize the importance of donor-acceptor dyads for effective separation and utilization of photoexcited charge carriers in efficient photocatalytic processes.

ASSOCIATED CONTENT

Supporting Information. The provided supporting information contains details on materials synthesis, catalytic conditions, further experimental results, further analytical data as well as the visualized computational data.

AUTHOR INFORMATION

Corresponding Author

*Michael J. Bojdys – Institut für Chemie, Humboldt-Universität zu Berlin, Brook-Taylor-Str. 2, 12489 Berlin, Germany; Department of Chemistry, King's College London, Britannia House Guy's Campus, 7 Trinity Street, London SE1 1DB, United Kingdom. Email: m.j.bojdys.02@cantab.net

*Matthias G. Trunk – Institut für Chemie, Humboldt-Universität zu Berlin, Brook-Taylor-Str. 2, 12489 Berlin, Germany. Email: matthias.trunk@gmail.com

Author Contributions

The manuscript was written through contributions of all authors. Matthias G. Trunk conceived the project, synthesized the materials, performed analytical work and wrote the paper. Guiping Li assisted in materials synthesis, analytical work, and performed the photocatalysis experiments. Hüseyin Küçükkeçeci performed SEM measurements and additional catalysis experiments. David Burmeister performed the DFT calculations. Martin Obermeier assisted in photocatalysis experiments. Boubacar Tanda Bonkano performed the TCSPC experiments. Arne Thomas assisted in evaluating the catalytic results and writing the paper. Matthias Schwalbe assisted in catalysis experiments and writing the paper. Michael J. Bojdys conceived the project and wrote the paper. All authors have given their approval to the final version of the manuscript.

Funding Sources

European Research Council (ERC) Starting Grant Scheme (BEGMAT-678462)

European Research Council (ERC) Proof of Concept Grant Scheme (LiAnMat-957534)

Einstein Center for Catalysis/Berlin International Graduate School for Natural Science and Engineering

Notes

The authors declare no conflict of interest.

ACKNOWLEDGMENTS

We thank Harald Link, and Christina Eichenauer of Berlin Institute of Technology for ICP-OES and TGA measurements, respectively. Thomas Dargel of Humboldt University of Berlin is acknowledged for support performing DFT calculations. H.K. thanks the Einstein Center for Catalysis/Berlin International Graduate School for Natural Science and Engineering for funding. M.J.B. thanks the European Research Council (ERC) for funding under the Starting Grant Scheme (BEGMAT-678462).

ABBREVIATIONS

SBP, sulfur and boron containing polymer; TAB, triarylborane; TT, thienothiophene; BDT, benzodithiophene; BT, bithiophene.

REFERENCES

(1) Wang, X.; Maeda, K.; Thomas, A.; Takanabe, K.; Xin, G.; Carlsson, J. M.; Domen, K.; Antonietti, M. A Metal-Free Polymeric Photocatalyst for Hydrogen Production from Water under Visible Light. *Nat. Mater.* **2009**, *8* (1), 76–80.

(2) Kochergin, Y. S.; Schwarz, D.; Acharjya, A.; Ichangi, A.; Kulkarni, R.; Eliášová, P.; Vacek, J.; Schmidt, J.; Thomas, A.; Bojdys, M. J. Exploring the "Goldilocks Zone" of Semiconducting Polymer Photocatalysts by Donor-Acceptor Interactions. *Angew. Chemie Int. Ed.* **2018**, *57* (43), 14188–14192.

(3) Yang, J.; Acharjya, A.; Ye, M. M.-Y.; Rabeah, J.; Li, S.; Kochovski, Z.; Youk, S.; Roeser, J.; Grüneberg, J.; Penschke, C.; Schwarze, M.; Wang, T.; Lu, Y.; Krol, R.; Oschatz, M.; Schomäcker, R.; Saalfrank, P.; Thomas, A. Protonated Imine-Linked Covalent Organic Frameworks for Photocatalytic Hydrogen Evolution. *Angew. Chemie Int. Ed.* **2021**, *60* (36), 19797–19803.

(4) Zwijnenburg, M. A.; Wu, Y.; Wang, X.; Sprick, R. S.; Little, M. A.; Zhu, W.-H.; Cooper, A. I.; Clowes, R.; Chen, L.; Chong, S. Y.; Yan, Y. Sulfone-Containing Covalent Organic Frameworks for Photocatalytic Hydrogen Evolution from Water. *Nat. Chem.* **2018**, *10* (12), 1180–1189.

(5) Schwarz, D.; Acharjya, A.; Ichangi, A.; Kochergin, Y. S.; Lyu, P.; Opanasenko, M. V.; Tarábek, J.; Vacek Chocholoušová, J.; Vacek, J.; Schmidt, J.; Čejka, J.; Nachtigall, P.; Thomas, A.; Bojdys, M. J. Tuning the Porosity and Photocatalytic Performance of Triazine-Based Graphdiyne Polymers through Polymorphism. *ChemSusChem* **2019**, *12* (1), 194–199.

(6) Cheng, J.; Tan, Z.-R.; Xing, Y.-Q.; Shen, Z.-Q.; Zhang, Y.; Liu, L.-L.; Yang, K.; Chen, L.; Liu, S.-Y. Exfoliated Conjugated Porous Polymer Nanosheets for Highly Efficient Photocatalytic Hydrogen Evolution. *J. Mater. Chem. A* **2021**, *9* (9), 5787–5795.

(7) Cheng, J.-Z.; Liu, L.-L.; Liao, G.; Shen, Z.-Q.; Tan, Z.-R.; Xing, Y.-Q.; Li, X.-X.; Yang, K.; Chen, L.; Liu, S.-Y. Achieving an Unprecedented Hydrogen Evolution Rate by Solvent-Exfoliated CPP-Based Photocatalysts. *J. Mater. Chem. A* **2020**, *8* (12), 5890–5899.

(8) Schwarz, D.; Acharjya, A.; Ichangi, A.; Lyu, P.; Opanasenko, M. V.; Goßler, F. R.; König, T. A. F.; Čejka, J.; Nachtigall, P.; Thomas, A.; Bojdys, M. J. Fluorescent Sulphur- and Nitrogen-Containing Porous Polymers with Tuneable Donor–Acceptor Domains for Light-Driven Hydrogen Evolution. *Chem. – A Eur. J.* **2018**, *24* (46), 11916–11921.

(9) Vyas, V. S.; Haase, F.; Stegbauer, L.; Savasci, G.; Podjaski, F.; Ochsenfeld, C.; Lotsch, B. V. A Tunable Azine Covalent Organic Framework Platform for Visible Light-Induced Hydrogen Generation. *Nat. Commun.* **2015**, *6* (1), 8508.

(10) Kuecken, S.; Acharjya, A.; Zhi, L.; Schwarze, M.; Schomäcker, R.; Thomas, A. Fast Tuning of Covalent Triazine Frameworks for Photocatalytic Hydrogen Evolution. *Chem. Commun.* **2017**, *53* (43), 5854–5857.

(11) Schwinghammer, K.; Hug, S.; Mesch, M. B.; Senker, J.; Lotsch, B. V. Phenyl-Triazine Oligomers for Light-Driven Hydrogen Evolution. *Energy Environ. Sci.* **2015**, *8* (11), 3345–3353.

(12) Kailasam, K.; Schmidt, J.; Bildirir, H.; Zhang, G.; Blechert, S.; Wang, X.; Thomas, A. Room Temperature Synthesis of Heptazine-Based Microporous Polymer Networks as Photocatalysts for Hydrogen Evolution. *Macromol. Rapid Commun.* **2013**, *34* (12), 1008–1013.

(13) Kailasam, K.; Mesch, M. B.; Möhlmann, L.; Baar, M.; Blechert, S.; Schwarze, M.; Schröder, M.; Schomäcker, R.; Senker, J.; Thomas, A. Donor-Acceptor-Type Heptazine-Based Polymer Networks for Photocatalytic Hydrogen Evolution. *Energy Technol.* **2016**, *4* (6), 744–750.

(14) Sharma, N.; Kumar, S.; Battula, V. R.; Kumari, A.; Giri, A.; Patra, A.; Kailasam, K. A Tailored Heptazine-Based Porous Polymeric Network as a Versatile Heterogeneous (Photo)Catalyst. *Chem. – A Eur. J.* **2021**, chem.202100595.

(15) Kochergin, Y. S.; Noda, Y.; Kulkarni, R.; Škodáková, K.; Tarábek, J.; Schmidt, J.; Bojdys, M. J. Sulfur- and Nitrogen-Containing Porous Donor–Acceptor Polymers as Real-Time Optical and Chemical Sensors. *Macromolecules* **2019**, *52* (20), 7696–7703.

(16) Sprick, R. S.; Bonillo, B.; Clowes, R.; Guiglion, P.; Brownbill, N. J.; Slater, B. J.; Blanc, F.; Zwijnenburg, M. A.; Adams, D. J.; Cooper, A. I. Visible-Light-Driven Hydrogen Evolution Using Planarized Conjugated Polymer Photocatalysts. *Angew. Chemie Int. Ed.* **2016**, *55* (5), 1792–1796.

(17) Wang, Z.; Yang, X.; Yang, T.; Zhao, Y.; Wang, F.; Chen, Y.; Zeng, J. H.; Yan, C.; Huang, F.; Jiang, J.-X. Dibenzothiophene Dioxide Based Conjugated Microporous Polymers for Visible-Light-Driven Hydrogen Production. *ACS Catal.* **2018**, *8* (9), 8590–8596.

(18) Vogel, A.; Forster, M.; Wilbraham, L.; Smith, C. L.; Cowan, A. J.; Zwijnenburg, M. A.; Sprick, R. S.; Cooper, A. I. Photocatalytically Active Ladder Polymers. *Faraday Discuss.* **2019**, *215*, 84–97.

(19) Han, C.; Dong, P.; Tang, H.; Zheng, P.; Zhang, C.; Wang, F.; Huang, F.; Jiang, J.-X. Realizing High Hydrogen Evolution Activity under Visible Light Using Narrow Band Gap Organic Photocatalysts. *Chem. Sci.* **2021**, *12* (5), 1796–1802.

(20) Turkoglu, G.; Cinar, M. E.; Ozturk, T. Triarylborane-Based Materials for OLED Applications. *Molecules* **2017**, *22* (9), 1522.

(21) Liu, X.; Zhang, Y.; Li, H.; A, S.; Xia, H.; Mu, Y. Triarylboron-Based Fluorescent Conjugated Microporous Polymers. *RSC Adv.* **2013**, *3* (44), 21267–21270.

(22) Zhao, W.; Zhuang, X.; Wu, D.; Zhang, F.; Gehrig, D.; Laquai, F.; Feng, X. Boron-π-Nitrogen-Based Conjugated Porous Polymers with Multi-Functions. *J. Mater. Chem. A* **2013**, *1* (44), 13878–13884.

(23) Suresh, V. M.; Bandyopadhyay, A.; Roy, S.; Pati, S. K.; Maji, T. K. Highly Luminescent Microporous Organic Polymer with Lewis Acidic Boron Sites on the Pore Surface: Ratiometric Sensing and Capture of F-Ions. *Chem. Eur. J.* **2015**, *21* (30), 10799–10804.

(24) Li, Z.; Li, H.; Xia, H.; Ding, X.; Luo, X.; Liu, X.; Mu, Y. Triarylboron-Linked Conjugated Microporous Polymers: Sensing and Removal of Fluoride Ions. *Chem. Eur. J.* **2015**, *21* (48), 17355–17362.

(25) Gu, C.; Huang, N.; Chen, Y.; Zhang, H.; Zhang, S.; Li, F.; Ma, Y.; Jiang, D. Porous Organic Polymer Films with Tunable Work Functions and Selective Hole and Electron Flows for Energy Conversions. *Angew. Chemie Int. Ed.* **2016**, *55* (9), 3049–3053.

(26) Dai, C.; Xu, S.; Liu, W.; Gong, X.; Panahandeh-Fard, M.; Liu, Z.; Zhang, D.; Xue, C.; Loh, K. P.; Liu, B. Dibenzothiophene- S , S -Dioxide-Based Conjugated Polymers: Highly Efficient Photocatalyts for Hydrogen Production from Water under Visible Light. *Small* **2018**, *14* (34), 1801839.

(27) Király, P. Background-Free Solution Boron NMR Spectroscopy. *Magn. Reson. Chem.* **2012**, *50* (9), 620–626.

(28) Bai, Y.; Wilbraham, L.; Slater, B. J.; Zwijnenburg, M. A.; Sprick, R. S.; Cooper, A. I. Accelerated Discovery of Organic Polymer Photocatalysts for Hydrogen Evolution from Water through the Integration of Experiment and Theory. *J. Am. Chem. Soc.* **2019**, *141* (22), 9063–9071.

(29) Jin, E.; Lan, Z.; Jiang, Q.; Geng, K.; Li, G.; Wang, X.; Jiang, D. 2D Sp2 Carbon-Conjugated Covalent Organic Frameworks for Photocatalytic Hydrogen Production from Water. *Chem* **2019**, *5* (6), 1632–1647.

(30) Biswal, B. P.; Vignolo-González, H. A.; Banerjee, T.; Grunenberg, L.; Savasci, G.; Gottschling, K.; Nuss, J.; Ochsenfeld, C.; Lotsch, B. V. Sustained Solar H 2 Evolution from a Thiazolo[5,4-d]Thiazole-Bridged Covalent Organic Framework and Nickel-Thiolate Cluster in Water. *J. Am. Chem. Soc.* **2019**, *141* (28), 11082–11092.

TABLE OF CONTENTS